ELSEVIER

Contents lists available at ScienceDirect

Fish and Shellfish Immunology

journal homepage: www.elsevier.com/locate/fsi



Full length article

Selective autophagy receptor p62/SQSTM1 inhibits TBK1-IRF7 innate immune pathway in triploid hybrid fish

Zhenghao Li, Huijuan Zhong, Shuting Lv, Yiru Huang, Shuaibin Pei, Yingbing Wei, Hui Wu, Jun Xiao *, Hao Feng **

State Key Laboratory of Developmental Biology of Freshwater Fish, College of Life Science, Hunan Normal University, Changsha, 410081, China

ARTICLE INFO

Keywords: SQSTM1 TBK1 IRF7 SVCV Triploid fish

ABSTRACT

The production of type I interferon is tightly regulated to prevent excessive immune activation. However, the role of selective autophagy receptor SQSTM1 in this regulation in teleost remains unknown. In this study, we cloned the triploid fish SQSTM1 (3nSQSTM1), which comprises 1371 nucleotides, encoding 457 amino acids. qRT-PCR data revealed that the transcript levels of SQSTM1 in triploid fish were increased both *in vivo* and *in vitro* following spring viraemia of carp virus (SVCV) infection. Immunofluorescence analysis confirmed that 3nSQSTM1 was mainly distributed in the cytoplasm. Luciferase reporter assay results showed that 3nSQSTM1 significantly blocked the activation of interferon promoters induced by 3nMDA5, 3nMAVS, 3nTBK1, and 3nIRF7. Co-immunoprecipitation assays further confirmed that 3nSQSTM1 could interact with both 3nTBK1 and 3nIRF7. Moreover, upon co-transfection, 3nSQSTM1 significantly inhibited the antiviral activity mediated by TBK1 and IRF7. Mechanistically, 3nSQSTM1 decreased the TBK1 phosphorylation and its interaction with 3nIRF7, thereby suppressing the subsequent antiviral response. Notably, we discovered that 3nSQSTM1 also interacted with SVCV N and P proteins, and these viral proteins may exploit 3nSQSTM1 to further limit the host's antiviral innate immune responses. In conclusion, our study demonstrates that 3nSQSTM1 plays a pivotal role in negatively regulating the interferon signaling pathway by targeting 3nTBK1 and 3nIRF7.

1. Introduction

Type I interferons (IFN-I) are a group of cytokines that play a critical role in response to viral infections. When the viruses infect a cell, they trigger signaling cascades that ultimately lead to the production and secretion of IFN-I [1]. TANK-binding kinase 1 (TBK1) is a key enzyme involved in the activation of IFN-I signaling. It serves as a critical mediator of the signaling pathways that lead to the activation of transcription factors such as interferon regulatory factor 7 (IRF7). TBK1 phosphorylates IRF7, leading to its activation and subsequent translocation to the nucleus where it induces the transcription of IFN-I and other antiviral genes [2–4]. However, excessive production of interferon can also trigger autoimmune diseases, so the interferon signaling pathway is strictly regulated [5–7].

Autophagy is involved in host defense against bacterial and viral

infections to maintain immune homeostasis and prevent unwanted inflammation [8,9]. Sequestosome 1 (p62/SQSTM1) is a multifunctional scaffolding protein. It acts as a selective autophagy receptor that recognizes and binds ubiquitin molecule-tagged proteins. p62/SQSTM1 transports these tagged proteins into the autophagosome and facilitates their fusion with lysosomes. Through these actions, it participates in the autophagic process and regulates multiple signaling pathways [10]. SQSTM1 mainly possesses five structural domains, namely, the N-terminal Phox and Bem1 (PB1) domain, the ZZ zinc-finger domain (ZnF-ZZ), the EIR domain, the LC3-interacting region (LIR) domain, and the ubiquitin-associated (UBA) domain at the C-terminal. The PB1 domain mainly mediates oligomerization on its own or with other selective autophagy receptors. SQSTM1 interacts with the N-terminal arginylated cargo via its ZnF-ZZ domain. The EIR domain is a region that interacts with E2 ubiquitin ligase and is able to increase the affinity of

E-mail addresses: xiaojun2018@hunnu.edu.cn (J. Xiao), fenghao@hunnu.edu.cn (H. Feng).

^{*} Corresponding author. State Key Laboratory of Developmental Biology of Freshwater Fish, College of Life Science, Hunan Normal University, Changsha, 410081, China.

^{**} Co-corresponding author. State Key Laboratory of Developmental Biology of Freshwater Fish, College of Life Science, Hunan Normal University, Changsha, 410081, China.

Table 1
Primers used in the study.

Primer name	Primer Sequence	Primer information			
CDS					
3nSQSTM1-F	ATGTCGATGACAGTGAAA For 3nSQSTM1 CDS cloin				
3nSQSTM1-R	CTACTTCTGTGGGCCGGG	•			
Expression vector					
3nSQSTM1-F	ACTGACgctagcATGTCGATGACAGTGAAAGCT	For expression vector construction			
3nSQSTM1-R	ACTGACctcgagTTACTTCTGTGGGCCGGGTTT				
qRT-PCR					
q-3nSQSTM1-F	GTGGCTCCATAGGGCTTCTC				
q-3nSQSTM1-R	CACTGCCTTGGTCTTTCTGC				
q-SVCV-M-F	CGACCGCGCCAGTATTGATGGATAC				
q-SVCV-M-R	ACAAGGCCGACCCGTCAACAGAG				
q-SVCV-N-F	GGGTCTTTACAGAGTGGG				
q-SVCV-N-R	TTTGTGAGTTGCCGTTAC				
q-SVCV-P-F	AACAGGTATCGACTATGGAAGAGC				
q-SVCV-P-R	GATTCCTCTTCCCAATTGACTGTC				
q-SVCV-G-F	GATGACTGGGAGTTAGATGGC				
q-SVCV-G-R	ATGAGGGATAATATCGGCTTG				
q-epc Viperin -F	GCAAAGCGAGGGTTACGAC				
q-epc Viperin-R	CTGCCATTACTAACGATGCTGAC				
q-epc ISG15-F	TGATGCAAATGAGACCGTAGAT				
q-epc ISG15-R	CAGTTGTCTGCCGTTGTAAATC				

Table 2Comparison of vertebrate SQSTM1 homologues(%).

Species	Full-length sequence		Species	Full-length sequence	
	Identity	Similarity		Identity	Similarity
Triploid hybrid	100.0	100.0	Centrocercus urophasianus	44.8	57.7
Carassius gibelio	98.3	98.3	Lagopus muta	44.6	57.3
Cyprinus carpio	93.7	95.2	Bufo gargarizans	47.1	58.7
Megalobrama amblycephala	86.5	90.0	Anser cygnoides	44.7	58.9
Ctenopharyngodon idella	85.0	89.0	Dermochelys coriacea	45.1	57.5
Danio rerio	82.5	86.7	Rana temporaria	44.8	57.6
Ictalurus punctatus	69.5	80.0	Bufo bufo	46.0	57.7
Oncorhynchus mykiss	61.6	71.0	Macaca mulatta	45.6	57.3
Salmo salar	59.5	69.1	Taeniopygia guttata	45.2	57.5
Perca fluviatilis	56.6	66.8	Tyto alba	44.5	56.1
Lacerta agilis	47.3	61.2	Passer montanus	44.5	56.1
Malaclemys terrapin pileata	45.9	59.0	Corvus hawaiiensis	45.6	57.8
Xenopus tropicalis	47.1	58.6	Hirundo rustica	45.4	57.7
Trachemys scripta elegans	45.6	58.6	Orcinus orca	45.4	57.7
Varanus komodoensis	46.3	59.3	Mus musculus	45.0	57.0
Chelonia mydas	45.8	57.7	Bos taurus	44.2	56.3
Gallus gallus	45.7	58.3	Rattus norvegicus	44.9	58.0
Chelonoidis abingdonii	46.3	58.4	Acinonyx jubatus	44.3	56.9
Terrape necarolina triunguis	45.7	58.3	Ursus americanus	44.4	56.4
Xenopus laevis	46.2	58.8	Homo sapiens	45.4	57.2
Nanorana parkeri	45.2	59.0	Ursus arctos	44.0	55.8
Aquila chrysaetos hrysaetos	45.8	57.8	Pongo abelii	44.2	56.0

SQSTM1 for ubiquitin. The LIR domain is a region that interacts with LC3 or ATG8s. The UBA domain is mainly responsible for interbinding with ubiquitin molecules [10–13].

It has been reported that SQSTM1 is involved in regulating IFN signaling [14,15]. SQSTM1 can regulate host antiviral immune responses by modulating a series of immune factors, such as RIG-I, cGAS, MAVS, STING, and IRF3 [16–21]. For example, the mycotoxin patulin inhibits TLR-mediated immune responses via SQSTM1-dependent mitochondrial autophagy and suppresses activation of the RLR/MAVS signaling axis via SQSTM1 interaction with TRAF6 [22]. Additionally, leucine-rich repeat containing protein 25 (LRRC25) binds specifically to RIG-I during viral infection, thereby promoting the interaction of RIG-I and SQSTM1, degrading RIG-I degradation through selective autophagy pathways, and inhibiting type I interferon production [23]. Furthermore, leucine-rich repeat containing protein (LRRC59) modulates type I

interferon signaling by restraining the SQSTM1-mediated autophagic degradation of RIG-I [16]. It has been proven that the hereditary hemochromatosis protein (HFE) mediated MAVS autophagic degradation by binding to SQSTM1 [24]. In addition, SQSTM1 can be phosphorylated by TBK1 to direct ubiquitinated STING to autophagosomes for degradation, thereby blocking cGAS-STING signaling [25]. Besides, OTUD7B deubiquitinates SQSTM1 and promotes IRF3 degradation to regulate antiviral immune responses [26]. Nevertheless, the role of SQSTM1 in antiviral immunity in teleost fish has not been elucidated.

Triploid hybrid fish (3n = 150), which has a genetic advantage in disease resistance over its parents and was produced by crossing a male allotetraploid (4n = 200) with a female red crucian carp (2n = 100), offer a valuable model for studying antiviral mechanisms due to its unique genetic makeup and enhanced disease resistance [27-29]. In this study, to investigate the role of SQSTM1 in antiviral immunity in triploid

Table 3Genbank accession numbers of vertebrate SQSTM1 homologues.

Species	GenBank Accession	Species	GenBank
	Number		Accession
			Number
Mammals			
Homo sapiens	NP_003891.1	Trachemys scripta	XP_034634458.1
		elegans	
Macaca mulatta	NP_001253287.1	Chelonoidis	XP_032628146.1
		abingdonii	
Pongo abelii	XP_009239645.2	Terrapene carolina	XP_024055543.1
		triunguis	
Rattus	NP_787037.2	Malaclemys terrapin	XP_053892875.1
norvegicus	-	pileata	-
Mus musculus	NP_035148.1	Varanus	XP_044310365.1
		komodoensis	
Bos taurus	NP_788814.1	Lacerta agilis	XP_032996160.1
Ursus arctos	XP_026363500.3	Amphibians	
Acinonyx	XP_026932737.1	Xenopus tropicalis	AAH80326.1
jubatus			
Ursus	XP_045650948.1	Xenopus laevis	NP_001079920.1
americanus			
Orcinus orca	XP_004284096.1	Bufo bufo	XP_040296797.1
Birds		Bufo gargarizans	XP_044137045.1
Gallus gallus	XP_040538686.1	Rana temporaria	XP_040200921.1
Lagopus muta	XP_048816709.1	Nanorana parkeri	XP_018409942.1
Corvus	XP_048175382.1	Fishes	
hawaiiensis			
Anser cygnoides	XP_047913273.1	Triploid hybrid	
Taeniopygia	XP_002195682.4	Danio rerio	AHA93916.1
guttata			
Hirundo rustica	XP_039934279.1	Cyprinus carpio	XP_042593729.1
Centrocercus	XP_042682527.1	Salmo salar	NP_001133813.1
urophasianus			
Passer montanus	XP_039557355.1	Oncorhynchus	XP_021439759.2
		mykiss	
Tyto alba	XP_032862159.1	Perca fluviatilis	XP_039669435.1
Aquila	XP_029853968.1	Ictalurus punctatus	XP_017329106.1
chrysaetos			
chrysaetos		0 ' 11'	IID 050 100 05 5
Reptiles	VD 0404005045	Carassius gibelio	XP_052430681.1
Chelonia mydas	XP_043408524.1	Ctenopharyngodon	QIC54186.1
D 1 1	VD 040046050 3	idella	VD 0400000444
Dermochelys	XP_043346858.1	Megalobrama	XP_048032344.1
coriacea		amblycephala	

fish, we cloned and characterized the SQSTM1 homolog of triploid fish (3nSQSTM1). We observed a marked increase in 3nSQSTM1 mRNA expression following SVCV infection. Besides, 3nSQSTM1 potently inhibited the activation of IFN promoters stimulated by 3nMDA5, 3nMAVS, 3nTBK1, and 3nIRF7. Co-IP assays confirmed the interaction between 3nSQSTM1 and 3nTBK1, as well as 3nIRF7. Additionally, 3nSQSTM1 effectively inhibited the antiviral activity of these target proteins by attenuating the phosphorylation of TBK1 and hindering the binding between 3nTBK1 and 3nIRF7. Importantly, we found that 3nSQSTM1 is also associated with SVCV N and P proteins, indicating a potential mechanism for the virus to manipulate the host's innate antiviral responses through the exploitation of 3nSQSTM1. Taken together, our results provide novel insights into the regulatory relationship between the RLR signaling factors and selective autophagy receptors in the antiviral innate immune response of teleost fish.

2. Materials and methods

2.1. Cells, plasmids, and transfection

HEK293T cells, *Epithelioma Papulosum Cyprinid* (EPC) cells, and triploid fish caudal fin cells (3nFC) were kept in the lab. HEK293T was cultured at 37 $^{\circ}$ C with 5 $^{\circ}$ C CO₂; EPC and 3nFC were cultured at 26 $^{\circ}$ C with 5 $^{\circ}$ C CO₂. All cell lines were maintained in Dulbecco's Modified Eagle Medium (DMEM) (BaseIMedia, China) containing 10 $^{\circ}$ 6 fetal bovine serum, 2 mM L-glutamine, 100 U/ml penicillin, and 100 µg/ml

streptomycin.

The recombinant expression plasmid of Myc-3nSQSTM1 was constructed by linking the open reading frame (ORF) of 3nSQSTM1 to pcDNA5/FRT/TO fused with a Myc tag at the N-terminus. The other plasmids, including Flag-3nMDA5, Flag-3nMAVS, Flag-3nTBK1, Flag-3nIRF7, pRL-TK, Luci-DrIFN ϕ 1 (for zebrafish IFN ϕ 1 promoter transcription analysis) and Luci-eIFN (for EPC IFN promoter transcription analysis) were kept in the lab. All the primer sequences were referenced in Table 1.

For cell transfection, polyethylenimine (PEI) (Yeasen, China) was used for transfection according to the manufacturer's instructions. The cells were seeded 18–24 h before transfection and the culture medium was changed to fresh medium containing 2 % FBS before transfection. After 4–6 h of transfection, the medium was replaced with fresh medium containing 10 % FBS.

2.2. Virus production, infection, and titer detection

EPC cells in 10 cm dishes were infected with SVCV (strain 741). After 2–3 days of viral infection, when the cytopathic effect (CPE) reached 50 %, cells and supernatant were collected, which were repeatedly freeze-thawed three times and then filtered using a 0.45 μm filter. EPC cells were subsequently infected with a gradient dilution of the viral supernatant. 1–2 h after viral infection, the viral supernatant was replaced with the semi-solid medium containing methylcellulose and 2 % FBS. Plaques were counted 2–3 days after infection.

2.3. Quantitative real-time PCR (qRT-PCR)

The relative mRNA level of SVCV-associated proteins (M, N, P, and G) and interferon-stimulated genes (Viperin and ISG15) in SVCV-infected EPC cells were detected by qRT-PCR with the SYBR Green staining. The operation program is as follows: 1 cycle of 95 °C/10 min, 40 cycles of 95 °C/15 s, 60 °C/1 min. The $2^{-\triangle\triangle CT}$ method was used to analyze the data. The primer sequences are listed in Table 1.

2.4. Luciferase reporter assay

EPC cells in 24-well plates (2×10^5 cells/well) were co-transfected with recombinant expression plasmid (300 ng), pRL-TK (25 ng) and Luci-eIFN/Luci-DrIFN ϕ 1 (200 ng) for 24 h. Cells were then collected and lysed with PLB lysate, the results were finally determined according to the Dual-Luciferase Reporter Assay System kit (Promega, USA).

2.5. Immunoblotting (IB)

HEK293T cells or EPC cells were transfected with expression plasmid, and the cells were collected and lysed approximately 48 h later. The prepared whole cell lysate samples were separated by 10 % SDS-PAGE electrophoresis, and the proteins were subsequently transferred to 0.45 µm PVDF membranes. The membranes were then blocked by soaking them in 5 % skimmed milk and incubated with primary antibodies at 4 °C overnight. After washing the membranes three times with TBST, the membranes were incubated with secondary antibodies at room temperature for 1 h. Band visualization was achieved using the BCIP/NBT Alkaline Phosphatase Color Development Kit (Sigma). The following primary antibodies were used in IB assay: mouse monoclonal anti-Myc primary Ab (1:5000, Abmart); mouse monoclonal anti-Flag primary Ab (1:5000, Abmart); mouse monoclonal anti-EGFP primary Ab (1:5000, Abmart); mouse monoclonal anti-β-actin primary Ab (1:5000, Affinity); Mouse pan-phosphoserine monoclonal primary Ab (1:2000, Abbkine).

2.6. Immunofluorescence

HeLa cells in 24-well plates were transfected with plasmid Myc-

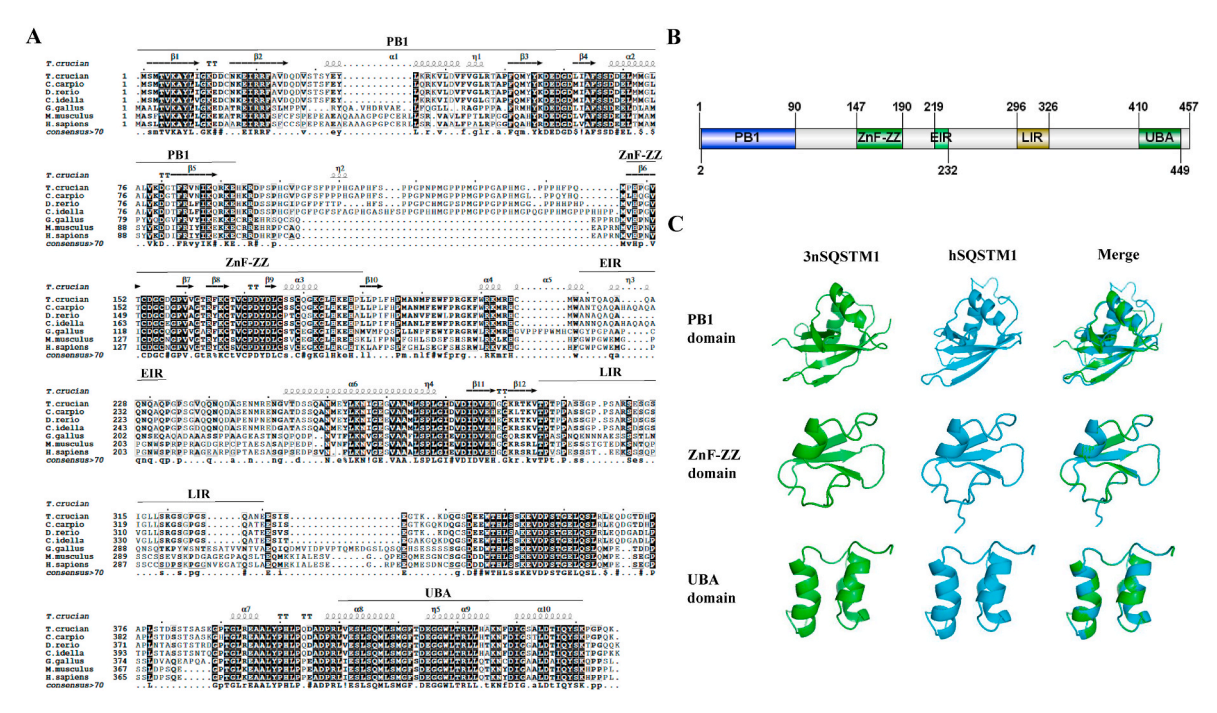
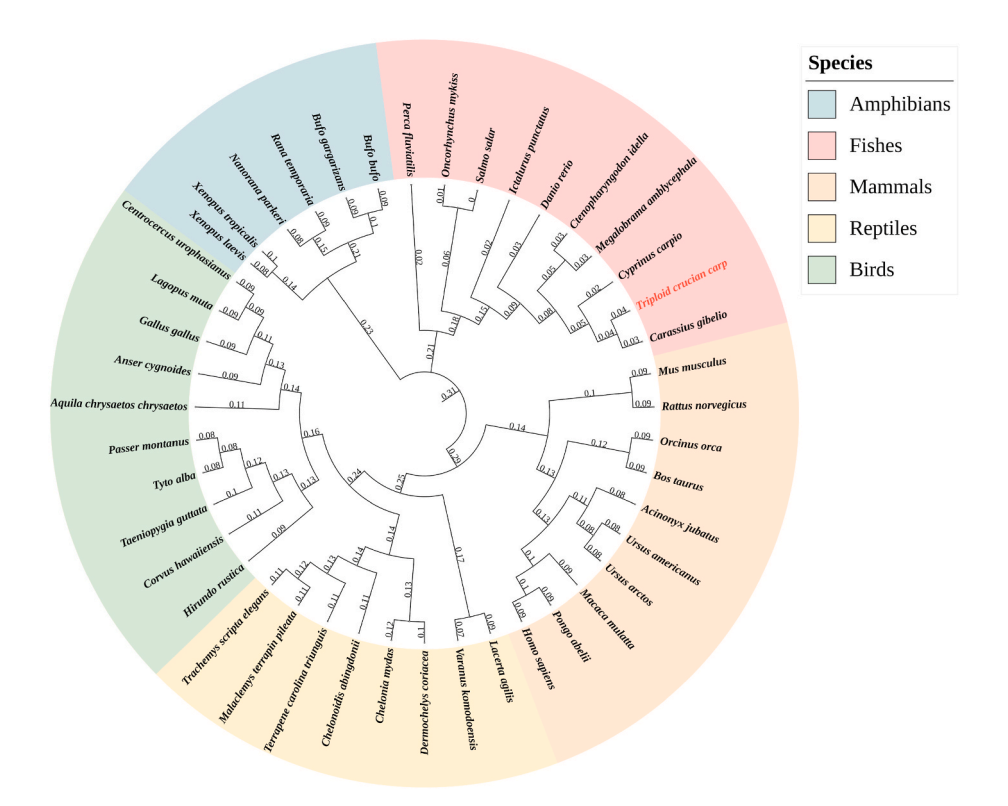


Fig. 1. Amino acid sequence analysis of 3nSQSTM1

(A) Amino acid multiple sequence alignments of SQSMT1 of *Homo sapiens* (NP_003891.1), *Mus musculus* (NP_035148.1), *Gallus gallus* (XP_040538686.1), *Ctenopharyngodon idella* (QIC54186.1), *Danio rerio* (AHA93916.1), and *Cyprinus carpio* (XP_042593729.1). (B) The main functional domain of 3nSQSTM1. PB1: N-terminal Phox and Bem1 domain. ZnF-Zz: Zz zinc-finger domain. LIR: LC3-interacting region domain. UBA: ubiquitin-associated domain. (C) The predicted 3D structure of 3nSQSTM1 by SMART (http://smart.embl-heidelberg.de/).



 $\textbf{Fig. 2.} \ \ \textbf{Phylogenetic evolutionary tree of SQSTM1} \ \ \textbf{in different vertebrates}$

The amino acid sequences of SQSTM1 were aligned for several species (GenBank accession numbers are listed in Table 3, the similarity and identity of these sequences are shown in Table 2). These species were categorized as mammals, birds, reptiles, amphibians, and fish. The results of the comparison were also constructed into a phylogenetic tree by neighbor-joining method using MEGA X, and the phylogenetic tree was annotated. Numbers on branches represent branch lengths.

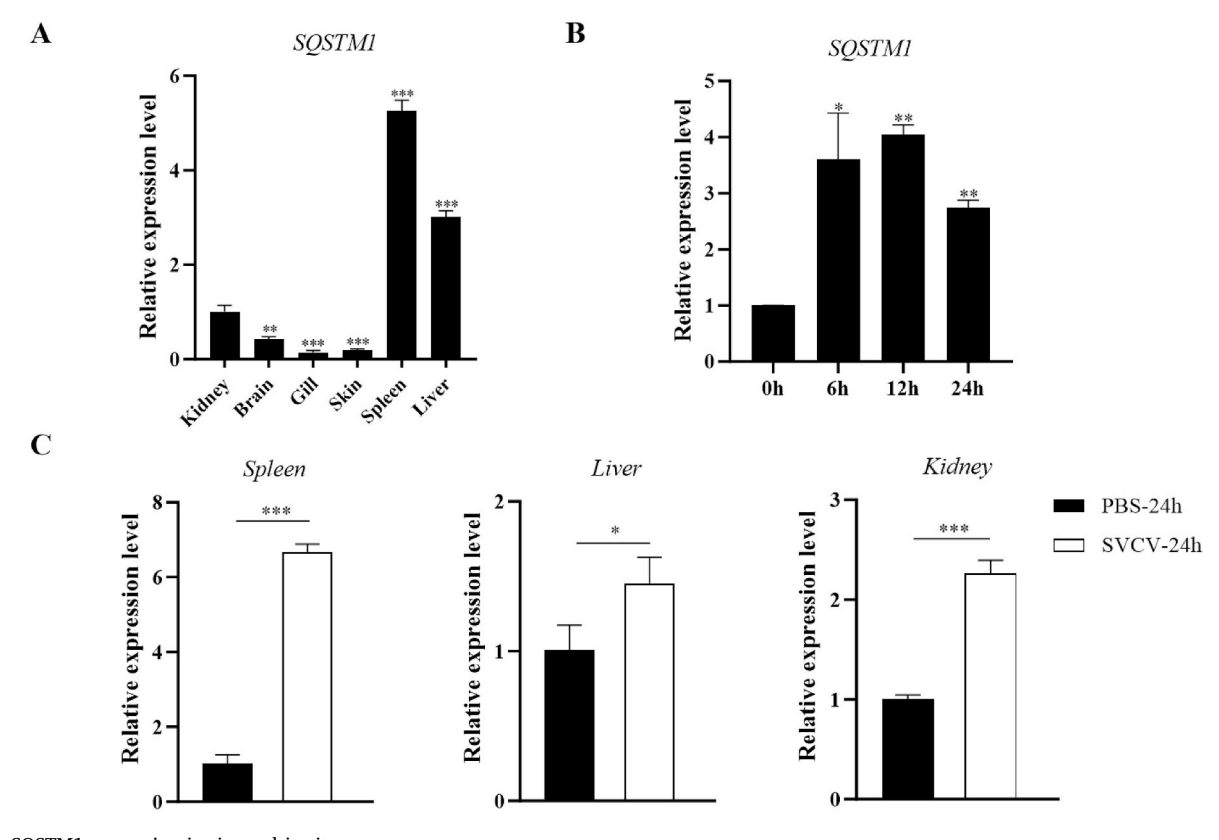


Fig. 3. 3nSQSTM1 expression *in vivo* and *in vitro*(A) Distribution of 3nSQSTM1 in different tissues of triploid hybrid. The mRNA level of 3nSQSTM1 in the kidney was used as a control. (B) The mRNA changes of 3nSQSTM1 in 3nFC at different time points of SVCV infection. (C) The triploid hybrid spleen, liver and kidney samples were taken at the same time 24 h after injection of PBS or SVCV, respectively, and tissue RNA was extracted, and qRT-PCR was performed to detect the changes in the 3nSQSTM1 content 24 h after viral infection, in which PBS was used as the control group.

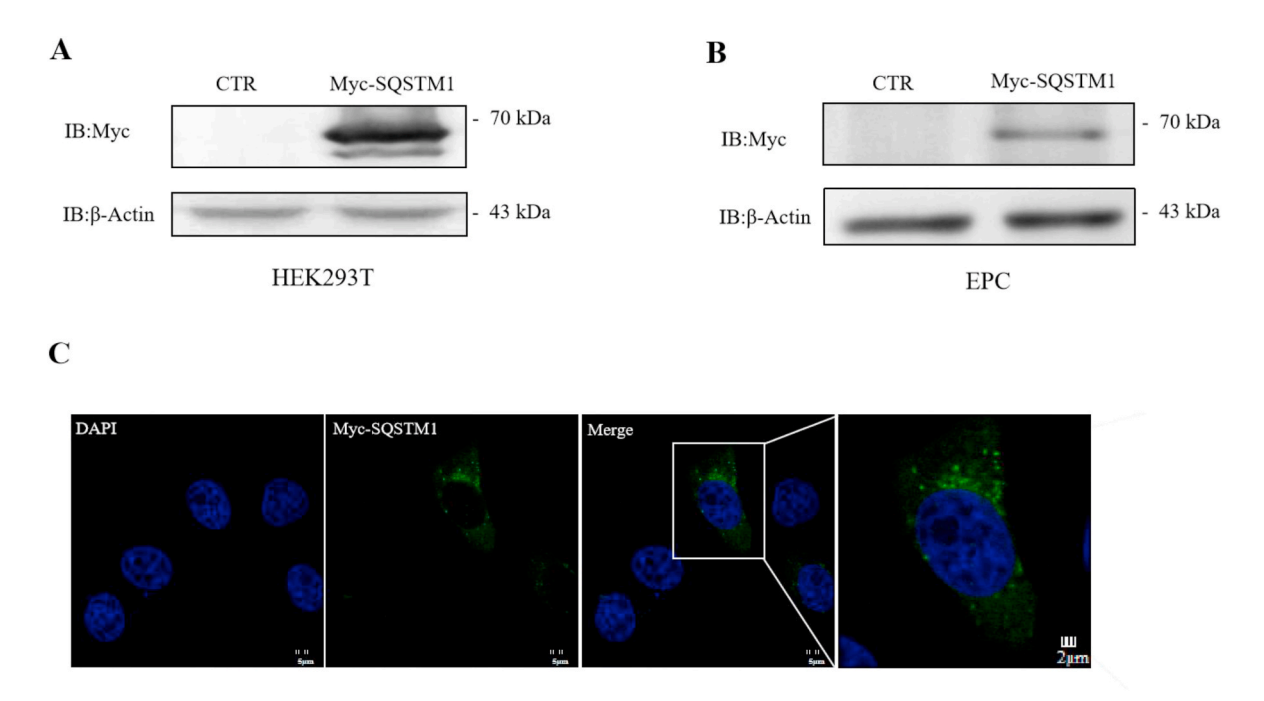


Fig. 4. Protein expression and intracellular distribution of 3nSQSTM1 Immunoblot (IB) assay of 3nSQSTM1 in HEK293T cells (A) and EPC cells (B). (C) The expression plasmid Myc-tagged 3nSQSTM1 was transfected into HeLa cells and the results were detected by immunofluorescence. DAPI: cell nuclear stain. the scale represents 10 µm and 2 µm, respectively.

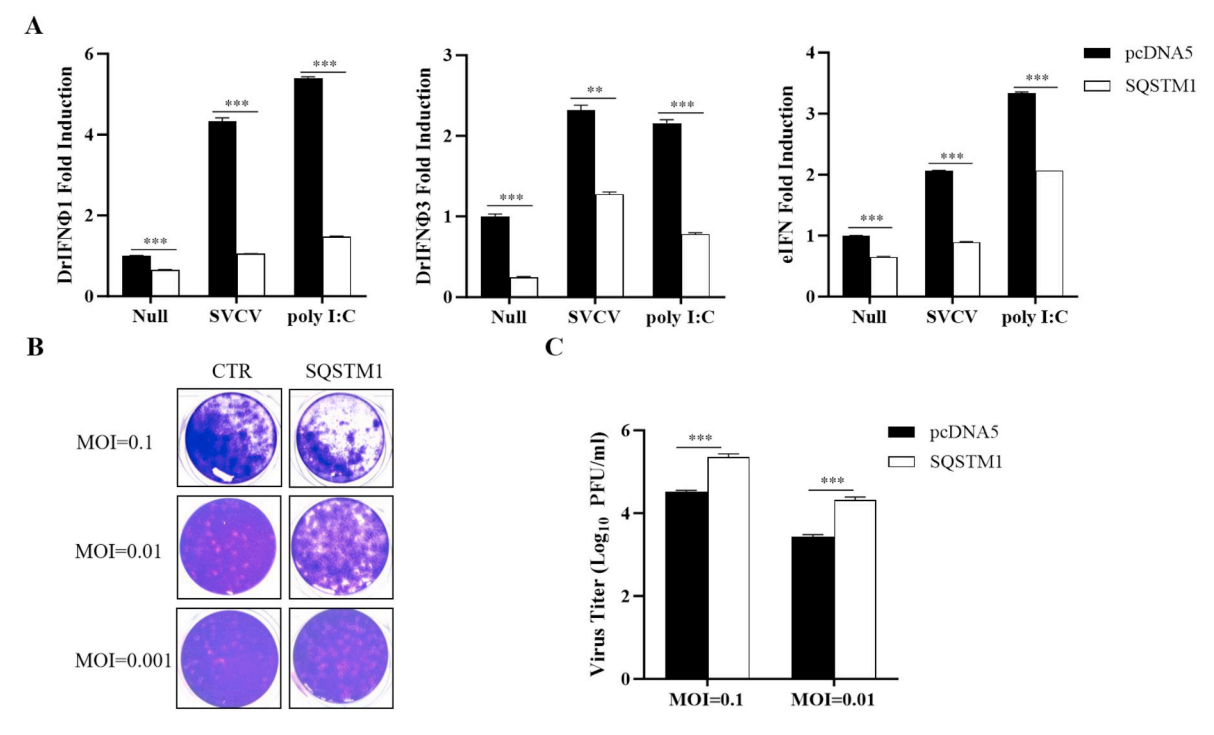


Fig. 5. 3nSQSTM1 negatively regulates cellular antiviral activity
(A) EPC cells were seeded in 24-well plates. The interferon promoter plasmids and TK plasmids were co-transfected with the empty vector for control and Myc-tagged 3nSQSTM1, respectively. Cells were stimulated with SVCV and poly(I:C) at 24 hpt, and subsequently subjected to luciferase reporter assay. The total amount of plasmid transfected in a single well was 525 ng. (B) At 24hp, cells were infected with SVCV and then replaced with semi-solid medium, and crystalline violet staining was performed. (C) The viral titers in the supernatants of SVCV-infected cells were detected at 24 hpi. Data represent the results of three independent experiments.

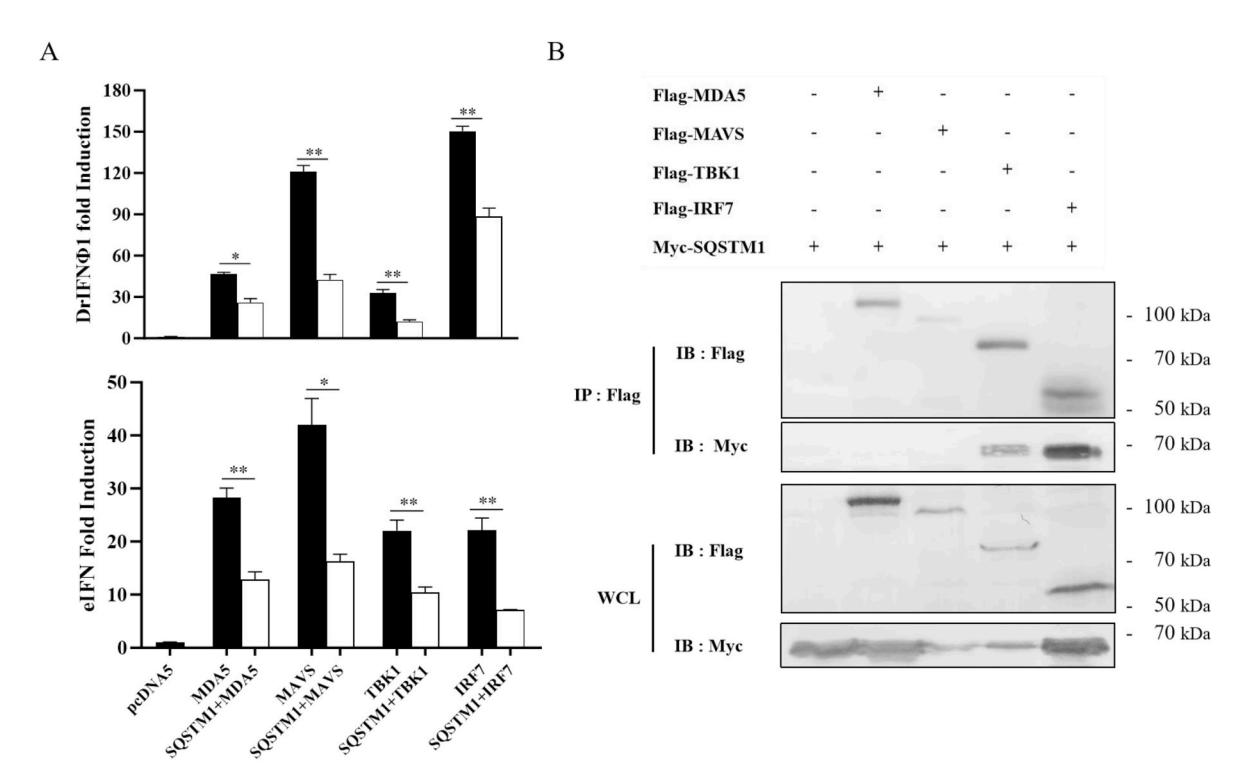


Fig. 6. 3nSQSTM1 interacts with 3nTBK1 and 3nIRF7

(A) EPC cells were seeded in 24-well plates and co-transfected with an interferon promoter plasmid and TK plasmid, together with 3nSQSTM1 and key adapter proteins from the RLR signaling pathway. Subsequently, a dual fluorescence assay was conducted. (B) Myc-tagged 3nSQSTM1 and Flag-tagged RLR factors were co-transfected into HEK293T cells, respectively. At 48 hpt, the cells were collected for immunoprecipitation experiments.

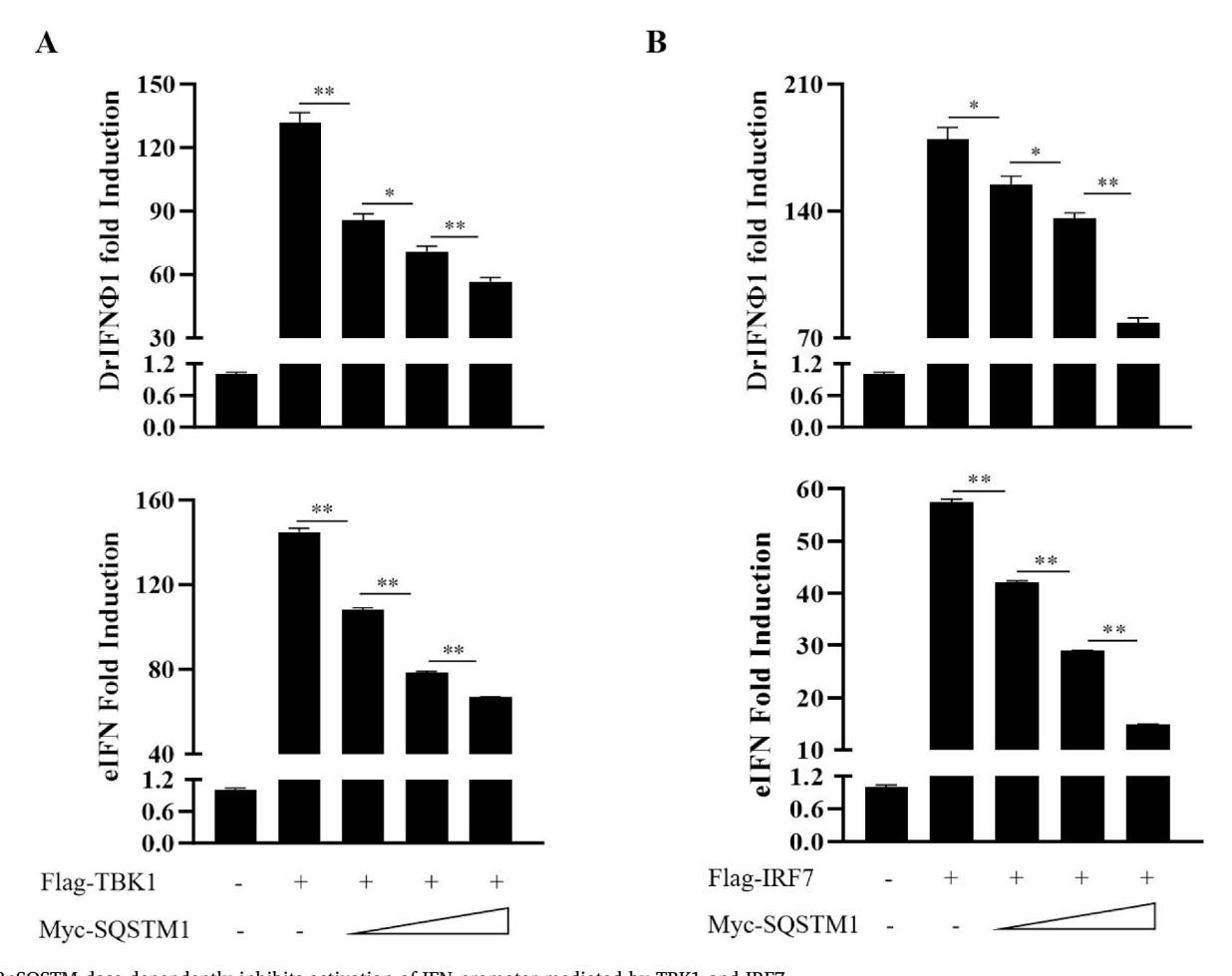


Fig. 7. 3nSQSTM dose-dependently inhibits activation of IFN promoter mediated by TBK1 and IRF7 (A&B) 24-well plates lined with EPC cells were transfected with Myc-tagged 3nSQSTM1(0 ng, 50 ng, 100 ng, or 200 ng) and equivalent doses of Flag-tagged 3nTBK1 (100 ng) (A) or Flag-tagged 3nIRF7 (100 ng) (B), and each well was simultaneously transfected with 25 ng of pRL-TK and 200 ng of the IFN promoter (DrIFN φ1). The total amount of transfected plasmids was balanced with the empty vector: pcDNA5/FRT/TO.

3nSQSTM1 (500 ng) for 24 h. Cells were subsequently fixed with 4 % paraformaldehyde for 10 min. The cells were immediately penetrated with 0.2 % Triton X-100 for 8 min and blocked with goat serum for 1 h. Next, the cells were sequentially incubated with mouse monoclonal anti-Myc primary Ab (1:500, Abmart) and Alexa Fluor 488-conjugated secondary Ab (1:1000, Invitrogen), respectively, for 1 h. Finally, the cells were washed five times with PBS. The coverslips were inverted onto slides, the nuclei were stained with drops of DAPI (H1200, Vector Laboratories) and sealed with nail polish. Slides were observed and photographed by using the laser confocal microscope (Olympus FV1200, Japan).

2.7. Immunoprecipitation (IP) and Co-immunoprecipitation (Co-IP)

The desired target plasmids were co-transfected in HEK293T cells and the cells were harvested 48h after transfection. Whole-cell lysates were obtained by centrifugation of the lysed and ultrasonically fragmented solutions. Whole-cell lysates were co-incubated with protein A/G agarose beads for 1-2 h at 4 °C, and then co-incubated with anti-HA-conjugated protein A/G agarose beads at 4 °C overnight. Finally, the beads were washed 5 times by centrifugation with 1 % NP40 solution, the beads were prepared for sampling and the results were detected by IB.

2.8. Statistics analysis

All data were obtained from three independent experiments, each in

triplicate. Error bars indicate the standard error of the mean (+SEM) of three independent experiments. Asterisk (*) stands for p <0.05, and (**) stands for p <0.01.

3. Results

3.1. Amino acid sequence analysis of 3nSQSTM1

To investigate the role of SQSTM1 in the antiviral innate immunity of triploid hybrid, the complete coding sequence (CDS) of 3nSQSTM1 (NCBI accession number: PP738648) has been cloned from the spleen of the triploid hybrid. The CDS of 3nSQSTM1 contains 1371 nucleotides and encodes 457 amino acids (Supplementary Fig. 1). The calculated molecular weight of 3nSQSTM1 is about 50 kDa and the predicted isoelectric point is 5.58 (by Expasy Compute PI/Mw). To understand the sequence conservation of SQSTM1 in vertebrates, the amino acid sequence of 3nSQSTM1 is used for multiple alignments with other vertebrate species, including Homo sapiens, Mus musculus, Gallus gallus, Ctenopharyngodon idella, Danio rerio, and Cyprinus carpio (Fig. 1A). The 3nSQSTM1 protein contains five major structural domains, including PB1, ZnF-ZZ, EIR, LIR, and UBA (Fig. 1B). The predicted 3D structure generated by SWISS-MODEL (https://swissmodel.expasy.org/) shows that the key functional domains of 3nSQSTM1 and hSQSTM1 share notable structural similarities, suggesting potential functional parity (Fig. 1C). To explore the evolutionary history of SQSTM1 across vertebrate lineages, we selected sequences of SQSTM1 from multiple species to construct a phylogenetic tree, including mammals, birds, reptiles,

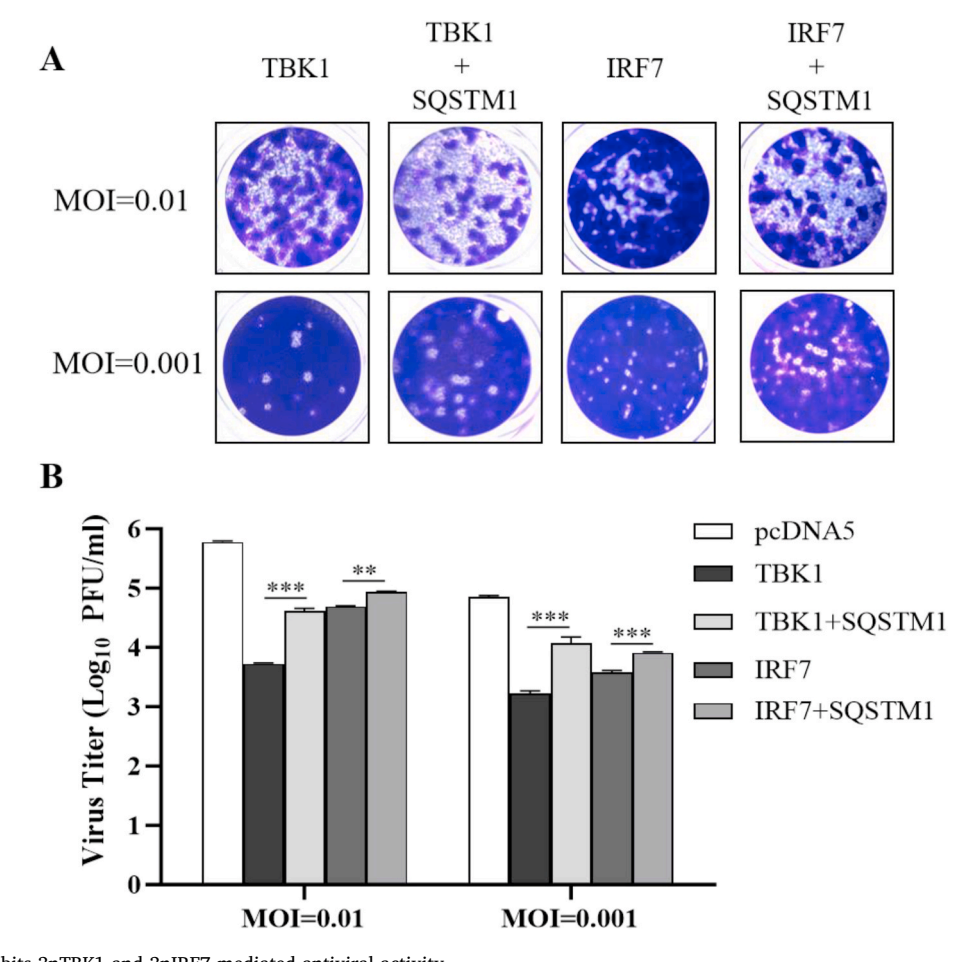


Fig. 8. 3nSQSTM1 inhibits 3nTBK1 and 3nIRF7 mediated antiviral activity
(A) EPC cells in 24-well plates were transfected with Flag-tagged 3nTBK1 and Flag-tagged 3nIRF7 alone or together with Myc-tagged 3nSQSTM1 at equal doses (250 ng each). At 24 hpt, cells were infected with SVCV, and after 1–2 h the medium was changed to semi-solid medium. Crystalline violet staining was performed to observe the cytopathic effect. (B) The viral titers in the supernatants of the EPC cells were detected at 24 hpi.

amphibians, and fishes. Phylogenetic analysis revealed conservation of SQSTM1 in teleost fish species, with 3nSQSTM1 grouping closely with SQSTM1 from *Carassius gibelio* and *Cyprinus carpio*, sharing 98 % and 94.1 % sequence identity, respectively (Fig. 2).

3.2. 3nSQSTM1 gene expression in vivo and in vitro

To explore the gene expression of 3nSQSTM1 in different tissues of triploid hybrid, we extracted total RNA from the brain, skin, gills, spleen, kidney, and liver. Using qRT-PCR, we noticed that 3nSQSTM1 is highly expressed in the spleen, liver and kidney (Fig. 3A). To gain more insight into the transcription of 3nSQSTM1 following infection, we evaluated the mRNA level of 3nSQSTM1 in 3nFC after SVCV infection. The results demonstrated a gradual increase in 3nSQSTM1 transcript levels within 24 h post-SVCV infection (Fig. 3B). Moreover, we examined the expression changes of 3nSQSTM1 in tissues after infection. The data revealed that, compared to the PBS-injected control group, 3nSQSTM1 exhibited significantly higher transcriptional levels in the spleen, liver, and kidney at the 24-h time point following SVCV injection (Fig. 3C). In conclusion, the above results suggest that 3nSQSTM1 may play a role in the host antiviral immune response to SVCV infection.

3.3. Protein expression and distribution of 3nSQSTM1

To investigate 3nSQSTM1 protein expression and distribution, we utilized the Myc-tagged 3nSQSTM1 plasmid for overexpression in HEK293T and EPC cells. The IB assay confirmed the successful

expression of the 3nSQSTM1 protein in both cell lines and specific bands of uniform size were detected (Fig. 4A and B). Subsequently, we aimed to detect the intracellular distribution of 3nSQSTM1 protein. We overexpressed the plasmid into HeLa cells and detected the protein's distribution by immunofluorescence. The results showed that 3nSQSTM1 was mainly distributed in the cytoplasm rather than in the nucleus (Fig. 4C).

3.4. 3nSQSTM1 negatively regulates cellular antiviral ability

To evaluate the effect of 3nSQSTM1 on cellular antiviral capacity, we initially examined its effect on the transcriptional activity of the IFN promoters, including zebrafish IFN ϕ 1 (DrIFN ϕ 1), zebrafish IFN ϕ 3 (DrIFN ϕ 3) and EPC IFN (eIFN). The results showed that 3nSQSTM1 was able to inhibit the activation of different interferon promoters, both under basal conditions and after stimulation (Fig. 5A). We next examined the effect of 3nSQSTM1 on cellular resistance to SVCV invasion and replication using crystal violet staining and viral titer assay. Our findings suggest that 3nSQSTM1 enhances SVCV invasion and replication within cells (Fig. 5B and C). In conclusion, the above data suggest that overexpression of 3nSQSTM1 attenuates the anti-SVCV capacity of the cells.

3.5. Interaction of 3nSQSTM1 with 3nTBK1 and 3nIRF7

The RLR/IFN signaling pathway is important for host innate immune responses against RNA viruses. To investigate the impact of 3nSQSTM1 on this pathway, we co-transfected 3nSQSTM1 with RLR signaling factors into EPC cells and performed luciferase reporter assays.

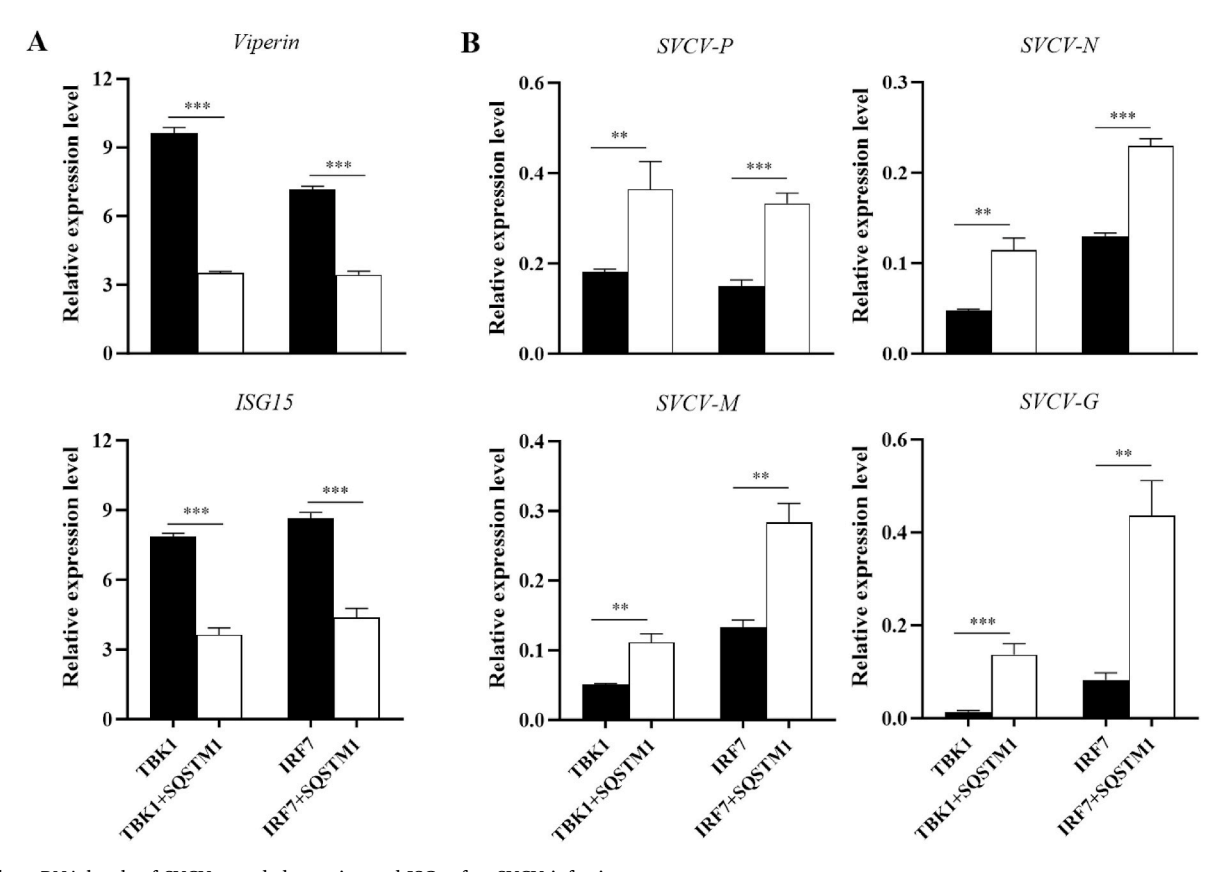


Fig. 9. The mRNA levels of SVCV encoded proteins and ISGs after SVCV infection (A&B) Collect the EPC cells corresponding to Fig. 8 and use them for RNA extraction. The mRNA transcript levels of ISGs (A) and SVCV-encoded proteins (B) were detected by qRT-PCR, respectively.

Interestingly, our findings revealed that 3nSQSTM1 effectively suppressed the activity of the zebrafish and EPC IFN promoters stimulated by these selected factors (Fig. 6A). Subsequently, we aimed to identify potential target proteins for 3nSQSTM1. To achieve this, we cotransfected the aforementioned plasmids into HEK293T cells and utilized co-IP assays. The results demonstrated that 3nSQSTM1 could interact with both 3nTBK1 and 3nIRF7 (Fig. 6B).

3.6. 3nSQSTM1 downregulates the antiviral activity of 3nTBK1 and 3nIRF7

To validate the above findings, we co-transfected 3nSQSTM1 with 3nTBK1 or 3nIRF7 into EPC cells, respectively. Dual fluorescence assay results indicated that 3nSQSTM1 was able to repress the transcriptional activity of the interferon promoters induced by 3nTBK1 and 3nIRF7 in a dose-dependent manner (Fig. 7A and B). Additionally, we further cotransfected 3nSQSTM1 with 3nTBK1 and 3nIRF7 in EPC cells, followed by crystal violet staining and viral titer assay upon SVCV infection. The results demonstrated that 3nSQSTM1 significantly reduced the cell's ability to resist SVCV infection mediated by 3nTBK1 and 3nIRF7 (Fig. 8A and B). Furthermore, the qRT-PCR results demonstrated that 3nSQSTM1 downregulated the transcription of specific interferonstimulated genes and facilitated higher replication of viral proteins encoded by SVCV upon co-transfection with 3nTBK1 and 3nIRF7, respectively (Fig. 9A and B). In conclusion, our results indicate that 3nSQSTM1 inhibits the cellular antiviral capacity mediated by 3nTBK1 and 3nIRF7, thereby increasing SVCV replication in EPC cells.

3.7. 3nSQSTM1 attenuates phosphorylation of 3nTBK1 and weakens the interaction of 3nTBK1 with 3nIRF7

To delve into the mechanism by which 3nSQSTM1 inhibits the

antiviral activity of TBK1-IRF7 axis, we first assessed the impact of 3nSQSTM1 on the protein levels of 3nTBK1 and 3nIRF7. Western blot analysis demonstrated that the co-transfection of 3nSQSTM1 did not significantly alter the protein levels of either 3nTBK1 or 3nIRF7 (Fig. 10A and B). However, subsequent immunoprecipitation assays revealed that 3nSQSTM1 notably reduced the pan-serine phosphorylation of 3nTBK1 (Fig. 10C). This finding suggests an inhibitory effect of 3nSQSTM1 on 3nTBK1 activation. Further investigation into the interaction between 3nTBK1 and 3nIRF7 showed that 3nSQSTM1 impaired the binding of 3nTBK1 to 3nIRF7 (Fig. 10D). These results collectively indicate that 3nSQSTM1 inhibits the antiviral activity of the TBK1-IRF7 axis by reducing TBK1 phosphorylation and disrupting the TBK1-IRF7 interaction, thereby impeding downstream antiviral signaling.

3.8. Interaction of 3nSQSTM1 with SVCV-encoded proteins

Finally, we aimed to investigate the potential interaction between 3nSQSTM1 and viral proteins encoded by SVCV. The Flag-tagged SVCV-P, -N, and, -G proteins were co-transfected with the Myc-tagged 3nSQSTM1, while the Myc-tagged SVCV-M was co-transfected with the Flag-tagged 3nSQSTM1 into HEK293T cells, respectively. Subsequently, co-immunoprecipitation assays were performed to detect the associations among these proteins. The results demonstrated that 3nSQSTM1 was capable of interacting with SVCV-P and SVCV-N, but not with SVCV-M and -G (Fig. 11A and Supplementary Fig. 2). To further elucidate the functional implications of these interactions, we cotransfected 3nSQSTM1, TBK1, and IRF7 with SVCV-P and -N proteins, respectively. Luciferase reporter assays revealed that when 3nSQSTM1 was co-expressed with viral proteins, the inhibitory effect of 3nSQSTM1 on interferon promoter activity triggered by 3nTBK1 and 3nIRF7 was significantly enhanced (Fig. 11B). This finding suggests a synergistic effect between 3nSQSTM1 and SVCV proteins in limiting interferon

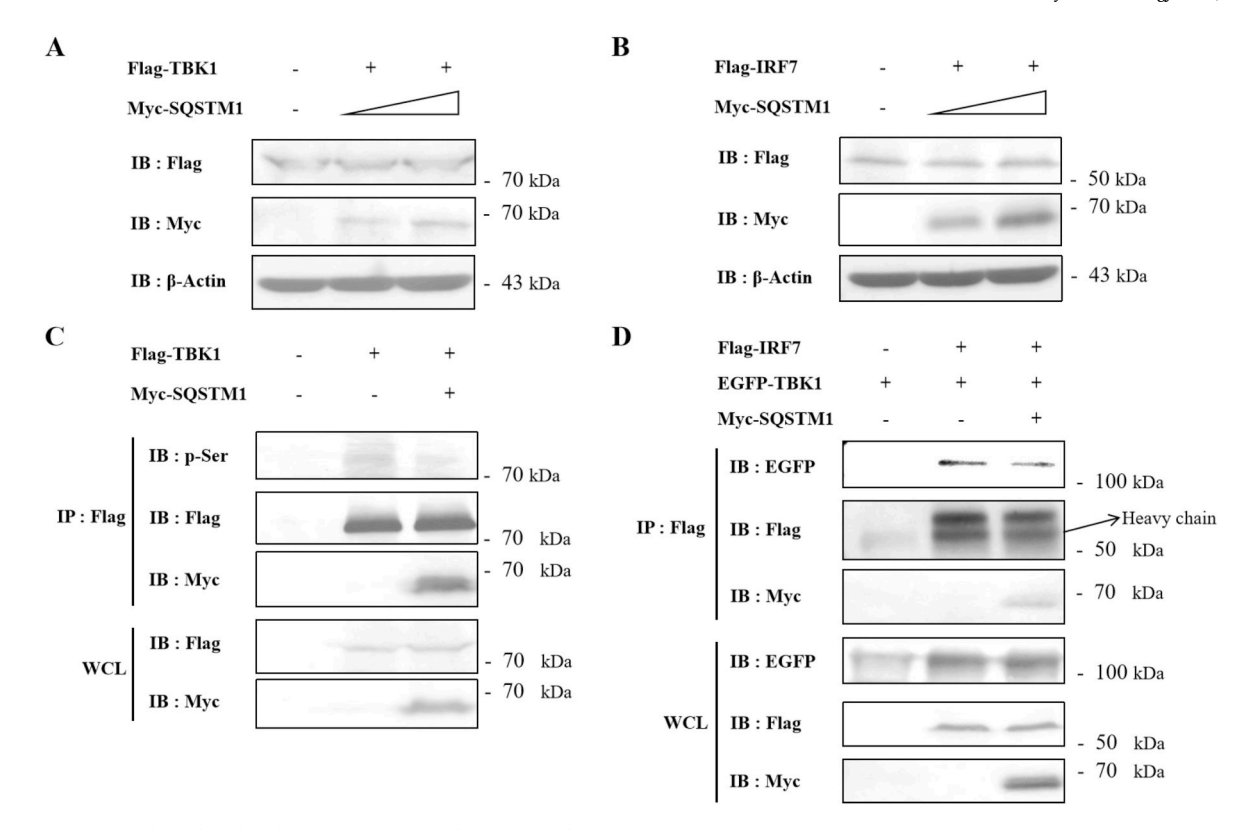


Fig. 10. 3nSQSTM1 inhibits phosphorylation of 3nTBK1 and attenuates the interaction of 3nTBK1 with 3nIRF7 (A&B) 6-well plates lined with EPC cells were transfected with Myc-tagged 3nSQSTM1(1 μg or 2 μg) and equivalent doses of Flag-tagged 3nTBK1 (2 μg) or Flag-tagged 3nIRF7 (2 μg). At 48 hpt, the cells were collected for WB. (C) Myc-tagged 3nSQSTM1 and Flag-tagged 3nTBK1 were co-transfected into HEK293T cells, respectively. At 48 hpt, the cells were collected for IP. (D) Myc-tagged 3nSQSTM1 with EGFP-tagged 3nTBK1 and Flag-tagged 3nIRF7 were co-transfected into HEK293T cells, respectively. At 48 hpt, the cells were collected for IP.

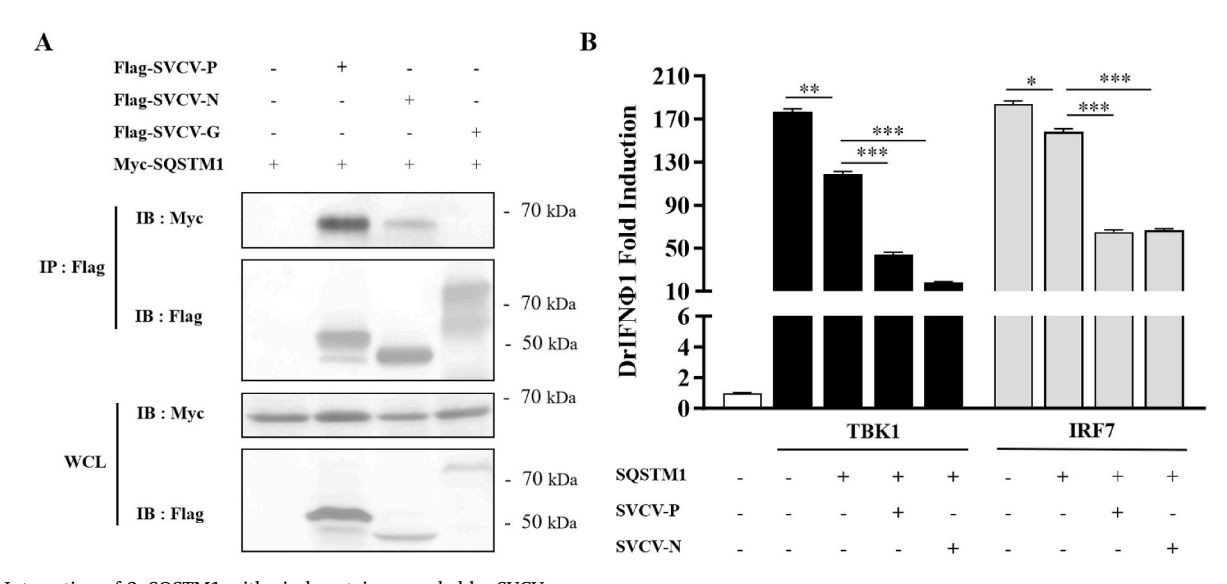


Fig. 11. Interaction of 3nSQSTM1 with viral proteins encoded by SVCV

(A) The Myc-tagged 3nSQSTM1 plasmid and the Flag-tagged SVCV-encoding genes were transfected into HEK293T cells, respectively. At 48 hpt, the cells were collected for immunoprecipitation experiments. (B) EPC cells were seeded in 24-well plates and co-transfected with an interferon promoter plasmid and TK plasmid, along with 3nSQSTM1 and SVCV-encoded P and N proteins, in the presence of TBK1 and IRF7, respectively. Dual fluorescence assay was then conducted on the transfected cells, and luciferase activity was measured 24h later.

production, which may have important implications for the pathogenesis of SVCV.

4. Discussion

IFN-I is a multifunctional cytokine, mainly composed of IFN- α and IFN- β , which plays an important role in regulating host antiviral immune responses [30]. IRF7 is a major regulator of the IFN-I immune

response, not only regulating the further expression of IFN- β but also triggering the production of IFN- α . The specific knockout of IRF7 in mouse pDCs almost loses the ability to produce IFN- α , and the deficiency of IRF7 in humans also significantly inhibits the production of IFN- α [31–34]. After infection of the host by pathogens such as viruses, through a series of intracellular signaling molecules, eventually the TBK1/IKK complex is able to activate the phosphorylation and dimerization of IRF3 and IRF7, which allows them to enter the nucleus to promote IFN-I expression [35]. The TBK1-IRF7-IFN-I axis plays a similar and important regulatory role in antiviral immunity in teleost fish [7, 36].

The results of the present study indicate that 3nSQSTM1, as a negative regulator, is able to further reduce the host's antiviral response capacity by inhibiting the TBK1-IRF7 axis. The autophagy pathway plays an important role in the regulation of host innate immunity [30, 37,38]. Previous research has shown that SQSTM1 can block signaling by directly binding to and degrading target proteins [16,21,25,39]. Additionally, it can indirectly degrade target proteins by binding to other proteins that target proteins, or by regulating its own activity through specific deubiquitinating enzymes or kinases [26]. We thus explored whether 3nSOSTM1 regulates the functions of 3nTBK1 and 3nIRF7 through degradation. Contrary to expectations, our data in Fig. 10A and B indicate that 3nSQSTM1 does not markedly alter the expression levels of 3nTBK1 and 3nIRF7. Instead, our results suggest that 3nSQSTM1 dampens the TBK1-IRF7 axis by inhibiting 3nTBK1 phosphorylation and disrupting the interaction between 3nTBK1 and 3nIRF7 (Fig. 10C and D). In mammals, SQSTM1 phosphorylated by TBK1 mediates the entry of ubiquitinated STING into the autophagosome for degradation, thereby inhibiting IFN signaling [25]. Further-OTUD7B deubiquitination of SQSTM1 promotes its oligomerization, thereby targeting IRF3 for autophagic degradation [26]. However, SQSTM1's role in IRF7 regulation has not been described. In conclusion, these findings in the present study diverge from the known mechanisms of SQSTM1 regulation on TBK1/IRF7 in mammals. Therefore, our study provides theoretical references and helps in disease resistance strategies in aquaculture at the molecular level.

Certain viruses have been shown to exploit the host's autophagic lysosomal degradation pathway. Their encoded proteins can bind to host proteins and utilize this pathway to degrade target proteins, thereby modulating the host's antiviral immunity and facilitating viral replication [40–42]. In this study, the co-IP results in Fig. 11 indicate that both N and P proteins encoded by SVCV interact with 3nSQSTM1. It is reasonable to speculate that these viral proteins are also likely to utilize the interaction with SQSTM1 to help the virus better antagonize the host's antiviral immune response. Further, luciferase reporter assay results suggest that when these viral proteins are present, the inhibitory effect of 3nSQSTM1 on interferon promoter activity is substantially augmented. This suggests that upon viral infection, these viral proteins may somehow hijack or assist SQSTM1 to further inhibit IFN signaling activated through TBK1 and IRF7. However, the specific regulatory mechanisms do not necessarily target TBK1 or IRF7 directly; for example, enhanced phosphorylation of SQSTM1 contributes to an increased affinity between SQSTM1 and ubiquitin chains, which in turn enhances the ability of SQSTM1 to degrade target proteins tagged with ubiquitin chains [25]. In addition, SQSTM1 can affect the stability of its own proteins by being deubiquitinated [43]. Overall, these viral proteins may alter the phosphorylation and ubiquitination levels of SQSTM1, which in turn can affect the expression or activity of SQSTM1. However, further experiments are necessary to elucidate the precise regulatory mechanism of these SVCV-encoded proteins on SQSTM1. Besides, it is also important to note that our study focuses exclusively on the SVCV and does not examine whether 3nSQSTM1 has similar effects on other types of viruses or pathogens. Expanding this research to include a broader range of pathogens would enhance our understanding of the general role of 3nSQSTM1 in the host's immune defense.

In summary, our research indicates that SQSTM1 can suppress the antiviral innate immune signaling triggered by TBK1 and IRF7 in triploid fish. SQSTM1's ability to inhibit the TBK1-IRF7 pathway and reduce interferon production likely serves as a fine-tuning mechanism to maintain immune homeostasis. By dampening the antiviral response once it has been adequately initiated, SQSTM1 helps to prevent an overzealous immune reaction that could harm the host. This balance ensures that while the fish are capable of mounting an effective defense against pathogens, the risk of autoimmunity and inflammatory damage is minimized. Thus, SQSTM1's role is not merely suppressive but is a crucial part of the regulatory network that maintains the health and resilience of the organism in the face of diverse pathogenic challenges. This discovery improves our comprehension of the role of autophagy-related proteins in regulating interferon-mediated antiviral responses.

CRediT authorship contribution statement

Zhenghao Li: Investigation, Writing – original draft. Huijuan Zhong: Investigation. Shuting Lv: Methodology. Yiru Huang: Visualization. Shuaibin Pei: Visualization. Yingbing Wei: Software. Hui Wu: Investigation. Jun Xiao: Writing-reviewing. Hao Feng: Supervision, Project administration, Writing – review & editing.

Data availability

Data will be made available on request.

Acknowledgements

This work was supported by the National Natural Science Foundation of China (31920103016, U21A20268, U22A20535, U23A20252), Hunan Provincial Science and Technology Department (2023JJ40435, 2023JJ10028), the Earmarked Fund for Hunan Agriculture Research System (HARS-06), Hunan Provincial Education Department (23B0070), the Research and Development Platform of Fish Disease and Vaccine for Post-graduates in Hunan Province.

Appendix A. Supplementary data

Supplementary data to this article can be found online at https://doi. org/10.1016/j.fsi.2024.109805.

References

- S. Akira, S. Uematsu, O. Takeuchi, Pathogen recognition and innate immunity, Cell 124 (2006) 783–801, https://doi.org/10.1016/j.cell.2006.02.015.
- [2] O. Takeuchi, S. Akira, Pattern recognition receptors and inflammation, Cell 140 (2010) 805–820, https://doi.org/10.1016/j.cell.2010.01.022.
- [3] Y. Zhang, J. Cen, G. Yuan, Z. Jia, K. Chen, W. Gao, J. Chen, M. Adamek, Z. Jia, J. Zou, DDX5 inhibits type I IFN production by promoting degradation of TBK1 and disrupting formation of TBK1 TRAF3 complex, Cell. Mol. Life Sci. 80 (2023) 212, https://doi.org/10.1007/s00018-023-04860-2.
- [4] H. Zhong, Q. Li, S. Pei, Y. Wu, Z. Li, X. Liu, Y. Peng, T. Zheng, J. Xiao, H. Feng, hnRNPM suppressed IRF7-mediated IFN signaling in the antiviral innate immunity in triploid hybrid fish, Dev. Comp. Immunol. 148 (2023) 104915, https://doi.org/ 10.1016/j.dci.2023.104915.
- [5] L.B. Nicholson, The immune system, Essays Biochem. 60 (2016) 275–301, https://doi.org/10.1042/EBC20160017.
- [6] C. Langevin, E. Aleksejeva, G. Passoni, N. Palha, J.-P. Levraud, P. Boudinot, The antiviral innate immune response in fish: evolution and conservation of the IFN system, J. Mol. Biol. 425 (2013) 4904–4920, https://doi.org/10.1016/j. imb.2013.09.033.
- [7] X.-Y. Gong, Q.-M. Zhang, J.-F. Gui, Y.-B. Zhang, SVCV infection triggers fish IFN response through RLR signaling pathway, Fish Shellfish Immunol. 86 (2019) 1058–1063, https://doi.org/10.1016/j.fsi.2018.12.063.
- [8] L.-F. Lu, Z.-C. Li, C. Zhang, D.-D. Chen, K.-J. Han, X.-Y. Zhou, X.-L. Wang, X.-Y. Li, L. Zhou, S. Li, Zebrafish TMEM47 is an effective blocker of IFN production during RNA and DNA virus infection, J. Virol. 97 (2023) e01434, https://doi.org/ 10.1128/jvi.01434-23, 23.
- [9] M.X. Chang, The negative regulation of retinoic acid-inducible gene I (RIG-I)-like receptors (RLRs) signaling pathway in fish, Dev. Comp. Immunol. 119 (2021) 104038, https://doi.org/10.1016/j.dci.2021.104038.

- [10] T. Lamark, S. Svenning, T. Johansen, Regulation of selective autophagy: the p62/ SQSTM1 paradigm, Essays Biochem. 61 (2017) 609–624, https://doi.org/10.1042/ EBC20170035
- [11] M. van der Vaart, C.J. Korbee, G.E.M. Lamers, A.C. Tengeler, R. Hosseini, M. C. Haks, T.H.M. Ottenhoff, H.P. Spaink, A.H. Meijer, The DNA damage-regulated autophagy modulator DRAM1 links mycobacterial recognition via TLR-MYD88 to autophagic defense, Cell Host Microbe 15 (2014) 753–767, https://doi.org/10.1016/j.chom.2014.05.005.
- [12] J.F. Gibson, T.K. Prajsnar, C.J. Hill, A.K. Tooke, J.J. Serba, R.D. Tonge, S.J. Foster, A.J. Grierson, P.W. Ingham, S.A. Renshaw, S.A. Johnston, Neutrophils use selective autophagy receptor Sqstm1/p62 to target Staphylococcus aureus for degradation in vivo in zebrafish, Autophagy 17 (2021) 1448–1457, https://doi.org/10.1080/ 15548627 2020 1765521
- [13] S.-J. Jeong, X. Zhang, A. Rodriguez-Velez, T.D. Evans, B. Razani, p62/SQSTM1 and selective autophagy in cardiometabolic diseases, Antioxid. Redox Signaling 31 (2019) 458–471, https://doi.org/10.1089/ars.2018.7649.
- [14] M.-H. Kung, Y.-S. Lin, T.-H. Chang, Aichi virus 3C protease modulates LC3- and SQSTM1/p62-involved antiviral response, Theranostics 10 (2020) 9200–9213, https://doi.org/10.7150/thpp.47077.
- [15] Y. Yu, C. Li, J. Liu, F. Zhu, S. Wei, Y. Huang, X. Huang, Q. Qin, Palmitic acid promotes virus replication in fish cell by modulating autophagy flux and TBK1-IRF3/7 pathway, Front. Immunol. 11 (2020) 1764, https://doi.org/10.3389/ fimmu 2020 01764
- [16] H. Xian, S. Yang, S. Jin, Y. Zhang, J. Cui, LRRC59 modulates type I interferon signaling by restraining the SQSTM1/p62-mediated autophagic degradation of pattern recognition receptor DDX58/RIG-I, Autophagy 16 (2020) 408–418, https://doi.org/10.1080/15548627.2019.1615303.
- [17] J. White, S. Suklabaidya, M.T. Vo, Y.B. Choi, E.W. Harhaj, Multifaceted roles of TAX1BP1 in autophagy, Autophagy 19 (2023) 44–53, https://doi.org/10.1080/ 15548627.2022.2070331.
- [18] W. Cao, J. Li, K. Yang, D. Cao, An overview of autophagy: mechanism, regulation and research progress, Bulletin Du Cancer 108 (2021) 304–322, https://doi.org/ 10.1016/j.bulcan.2020.11.004.
- [19] D.J. Klionsky, G. Petroni, R.K. Amaravadi, E.H. Baehrecke, A. Ballabio, P. Boya, J. M. Bravo-San Pedro, K. Cadwell, F. Cecconi, A.M.K. Choi, M.E. Choi, C.T. Chu, P. Codogno, M.I. Colombo, A.M. Cuervo, V. Deretic, I. Dikic, Z. Elazar, E.-L. Eskelinen, G.M. Fimia, D.A. Gewirtz, D.R. Green, M. Hansen, M. Jäättelä, T. Johansen, G. Juhász, V. Karantza, C. Kraft, G. Kroemer, N.T. Ktistakis, S. Kumar, C. Lopez-Otin, K.F. Macleod, F. Madeo, J. Martinez, A. Meléndez, N. Mizushima, C. Münz, J.M. Penninger, R.M. Perera, M. Piacentini, F. Reggiori, D.C. Rubinsztein, K.M. Ryan, J. Sadoshima, L. Santambrogio, L. Scorrano, H.-U. Simon, A.K. Simon, A. Simonsen, A. Stolz, N. Tavernarakis, S.A. Tooze, T. Yoshimori, J. Yuan, Z. Yue, Q. Zhong, L. Galluzzi, F. Pietrocola, Autophagy in major human diseases, EMBO J. 40 (2021) e108863, https://doi.org/10.15252/embj.2021108863.
- [20] S. Liu, S. Yao, H. Yang, S. Liu, Y. Wang, Autophagy: regulator of cell death, Cell Death Dis. 14 (2023) 648, https://doi.org/10.1038/s41419-023-06154-8.
- [21] Y. Wu, S. Jin, Q. Liu, Y. Zhang, L. Ma, Z. Zhao, S. Yang, Y.-P. Li, J. Cui, Selective autophagy controls the stability of transcription factor IRF3 to balance type I interferon production and immune suppression, Autophagy 17 (2021) 1379–1392, https://doi.org/10.1080/15548627.2020.1761653.
- [22] W.-T. Tsai, Y.-C. Lo, M.-S. Wu, C.-Y. Li, Y.-P. Kuo, Y.-H. Lai, Y. Tsai, K.-C. Chen, T.-H. Chuang, C.-H. Yao, J.-C. Lee, L.-C. Hsu, J.T.-A. Hsu, G.-Y. Yu, Mycotoxin patulin suppresses innate immune responses by mitochondrial dysfunction and p62/Sequestosome-1-dependent mitophagy, J. Biol. Chem. 291 (2016) 19299–19311, https://doi.org/10.1074/jbc.M115.686683.
- [23] Y. Du, T. Duan, Y. Feng, Q. Liu, M. Lin, J. Cui, R. Wang, LRRC25 inhibits type I IFN signaling by targeting ISG15-associated RIG-I for autophagic degradation, Embo J 37 (2018) 351–366, https://doi.org/10.15252/embj.201796781.
- [24] J. Liu, X. Wu, H. Wang, J. Wei, Q. Wu, X. Wang, Y. Yan, J. Cui, J. Min, F. Wang, J. Zhou, HFE inhibits type I IFNs signaling by targeting the SQSTM1-mediated MAVS autophagic degradation, Autophagy 17 (2021) 1962–1977, https://doi.org/10.1080/15548627.2020.1804683.
- [25] T. Prabakaran, C. Bodda, C. Krapp, B.-C. Zhang, M.H. Christensen, C. Sun, L. Reinert, Y. Cai, S.B. Jensen, M.K. Skouboe, J.R. Nyengaard, C.B. Thompson, R. J. Lebbink, G.C. Sen, G. van Loo, R. Nielsen, M. Komatsu, L.N. Nejsum, M. R. Jakobsen, M. Gyrd-Hansen, S.R. Paludan, Attenuation of cGAS-STING signaling

- is mediated by a p62/SQSTM1-dependent autophagy pathway activated by TBK1, EMBO J. 37 (2018) e97858, https://doi.org/10.15252/embj.201797858.
- [26] W. Xie, S. Tian, J. Yang, S. Cai, S. Jin, T. Zhou, Y. Wu, Z. Chen, Y. Ji, J. Cui, OTUD7B deubiquitinates SQSTM1/p62 and promotes IRF3 degradation to regulate antiviral immunity, Autophagy 18 (2022) 2288–2302, https://doi.org/10.1080/ 15548627.2022.2026098.
- [27] S. Chen, J. Wang, S. Liu, Q. Qin, J. Xiao, W. Duan, K. Luo, J. Liu, Y. Liu, Biological characteristics of an improved triploid crucian carp, Science in China, Series C, Life Sciences 52 (2009) 733–738, https://doi.org/10.1007/s11427-009-0079-3.
- [28] S. Liu, Distant hybridization leads to different ploidy fishes, Science China, Life Sci. 53 (2010) 416–425, https://doi.org/10.1007/s11427-010-0057-9.
- [29] J. Xiao, Y. Fu, W. Zhou, L. Peng, J. Xiao, S. Liu, H. Feng, Establishment of fin cell lines and their use to study the immune gene expression in cyprinid fishes with different ploidy in rhabdovirus infection, Dev. Comp. Immunol. 88 (2018) 55–64, https://doi.org/10.1016/j.dci.2018.07.007.
- [30] W. Ma, G. Huang, Z. Wang, L. Wang, Q. Gao, IRF7: role and regulation in immunity and autoimmunity, Front. Immunol. 14 (2023) 1236923, https://doi.org/10.3389/ fimmu.2023.1236923.
- [31] Q. Liang, H. Deng, C.-W. Sun, T.M. Townes, F. Zhu, Negative regulation of IRF7 activation by activating transcription factor 4 suggests a cross-regulation between the IFN responses and the cellular integrated stress responses, J. Immunol. 186 (2011) 1001–1010, https://doi.org/10.4049/jimmunol.1002240.
- [32] K. Honda, H. Yanai, H. Negishi, M. Asagiri, M. Sato, T. Mizutani, N. Shimada, Y. Ohba, A. Takaoka, N. Yoshida, T. Taniguchi, IRF-7 is the master regulator of type-I interferon-dependent immune responses, Nature 434 (2005) 772–777, https://doi.org/10.1038/nature03464.
- [33] G.L. Bentz, R. Liu, A.M. Hahn, J. Shackelford, J.S. Pagano, Epstein-Barr virus BRLF1 inhibits transcription of IRF3 and IRF7 and suppresses induction of interferon-β, Virology 402 (2010) 121–128, https://doi.org/10.1016/j. virol.2010.03.014.
- [34] B. Zhou, W. Yang, W. Li, L. He, L. Lu, L. Zhang, Z. Liu, Y. Wang, T. Chao, R. Huang, Y. Gu, T. Jia, Q. Liu, S. Tian, P. Pierre, T. Maeda, Y. Liang, E. Kong, Zdhhc2 is essential for plasmacytoid dendritic cells mediated inflammatory response in psoriasis, Front. Immunol. 11 (2021) 607442, https://doi.org/10.3389/fimmu.2020.607442.
- [35] K. Honda, T. Taniguchi, IRFs: master regulators of signalling by Toll-like receptors and cytosolic pattern-recognition receptors, Nat. Rev. Immunol. 6 (2006) 644–658, https://doi.org/10.1038/nri1900.
- [36] B. Collet, C.J. Secombes, Type I-interferon signalling in fish, Fish Shellfish Immunol. 12 (2002) 389–397, https://doi.org/10.1006/fsim.2001.0405.
- [37] U. Ashraf, Y. Lu, L. Lin, J. Yuan, M. Wang, X. Liu, Spring viraemia of carp virus: recent advances, J. Gen. Virol. 97 (2016) 1037–1051, https://doi.org/10.1099/ igv.0.000436.
- [38] S.N. Chen, P.F. Zou, P. Nie, Retinoic acid-inducible gene I (RIG-I)-like receptors (RLRs) in fish: current knowledge and future perspectives, Immunology 151 (2017) 16–25. https://doi.org/10.1111/jmm.12714.
- [39] D.H. Lee, J.S. Park, Y.S. Lee, J. Han, D.-K. Lee, S.W. Kwon, D.H. Han, Y.-H. Lee, S. H. Bae, SQSTM1/p62 activates NFE2L2/NRF2 via ULK1-mediated autophagic KEAP1 degradation and protects mouse liver from lipotoxicity, Autophagy 16 (2020) 1949–1973, https://doi.org/10.1080/15548627.2020.1712108.
- [40] T. Wang, R. Luo, J. Zhang, J. Lan, Z. Lu, H. Zhai, L.-F. Li, Y. Sun, H.-J. Qiu, The African swine fever virus MGF300-4L protein is associated with viral pathogenicity by promoting the autophagic degradation of IKKβ and increasing the stability of IκΒα, Emerg. Microb. Infect. (2024) 2333381 https://doi.org/10.1080/22221751 2004 2333381
- [41] J. Cao, M. Shi, L. Zhu, X. Li, A. Li, S.-Y. Wu, C.-M. Chiang, Y. Zhang, The matrix protein of respiratory syncytial virus suppresses interferon signaling via RACK1 association, J. Virol. 97 (2023) e0074723, https://doi.org/10.1128/jvi.00747-23.
- [42] J.W. Thinwa, Z. Zou, E. Parks, S. Sebti, K. Hui, Y. Wei, M. Goodarzi, V. Singh, G. Urquhart, J.L. Jewell, J.K. Pfeiffer, B. Levine, T.A. Reese, M.U. Shiloh, CDKL5 regulates p62-mediated selective autophagy and confers protection against neurotropic viruses, J. Clin. Invest. 134 (2024) e168544, https://doi.org/10.1172/ JCI168544.
- [43] H. Peng, F. Yang, Q. Hu, J. Sun, C. Peng, Y. Zhao, C. Huang, The ubiquitin-specific protease USP8 directly deubiquitinates SQSTM1/p62 to suppress its autophagic activity, Autophagy 16 (2020) 698–708, https://doi.org/10.1080/ 15548627.2019.1635381.